Excited-State Processes in the Carotenoid Zeaxanthin after Excess Energy Excitation

Helena Hörvin Billsten,[†] Jingxi Pan,[†,‡] Subrata Sinha,[†] Torbjörn Pascher,[†] Villy Sundström,[†] and Tomáš Polívka*[,†]

Department of Chemical Physics, Chemical Center, Lund University, Box 124, 22100 Lund, Sweden, and Department of Chemistry, The University of Western Ontario, London, Ontario, N6A 5B7, Canada

Received: April 29, 2005; In Final Form: June 13, 2005

Aiming for better understanding of the large complexity of excited-state processes in carotenoids, we have studied the excitation wavelength dependence of the relaxation dynamics in the carotenoid zeaxanthin. Excitation into the lowest vibrational band of the S_2 state at 485 nm, into the 0−3 vibrational band of the S_2 state at 400 nm, and into the $^2B_u^+$ state at 266 nm resulted in different relaxation patterns. While excitation at 485 nm produces the known four-state scheme ($S_2 \rightarrow$ hot $S_1 \rightarrow S_1 \rightarrow S_0$), excess energy excitation led to additional dynamics occurring with a time constant of 2.8 ps (400 nm excitation) and 4.9 ps (266 nm excitation), respectively. This process is ascribed to a conformational relaxation of conformers generated by the excess energy excitation. The zeaxanthin S* state was observed regardless of the excitation wavelength, but its population increased after 400 and 266 nm excitation, suggesting that conformers generated by the excess energy excitation are important for directing the population toward the S* state. The S_2-S_1 internal conversion time was shortened from 135 to 70 fs when going from 485 to 400 nm excitation, as a result of competition between the S_2-S_1 internal conversion from the vibrationally hot S_2 state and S_2 vibrational relaxation. The S_1 lifetime of zeaxanthin was within experimental error the same for all excitation wavelengths, yielding ∼9 ps. No long-lived species have been observed after excitation by femtosecond pulses regardless of the excitation wavelength, but excitation by nanosecond pulses at 266 nm generated both zeaxanthin triplet state and cation radical.

1. Introduction

Carotenoids are widely distributed natural pigments that have various functions in biological systems. In photosynthesis, carotenoids play important roles in light harvesting and photoprotection.[1,2] As light-harvesting agents, they capture sunlight in the blue-green region of the spectrum and transfer energy to (bacterio)chlorophylls.[1] The photoprotective function of carotenoids relies on their ability to intercept processes leading to a formation of reactive species by quenching both singlet and triplet states of (bacterio)chlorophylls. In these processes, carotenoid triplet states and carotenoid radicals play a key role.[3−5] Recent observations that carotenoid triplets[6,7] and radicals[8−13] can be formed on the ultrafast time scale in both natural[6−10] and artificial[11−13] photosynthetic systems have demonstrated that processes involving carotenoid triplets and radicals are not limited to slow time scales. Instead, ultrafast carotenoid radical formation has been suggested to be of importance for photoprotection in higher plants.[8]

Knowledge of carotenoid photophysics is a necessary prerequisite for understanding fine details of molecular actions of carotenoids. During the past decade, a vast number of experimental and theoretical studies have aimed at revealing the complicated picture of excited-state processes in carotenoids.[1] In addition to the well-known fact that the lowest excited state of carotenoids (S_1, $^2A_g^-$ in the notation of the C_{2h} symmetry group) is a dark state and the strong absorption is due to the transition from the S_0 ($^1A_g^-$) state to the S_2 state ($^1B_u^+$), existence of other dark states, such as $^3A_g^-$ and $^1B_u^-$,[14,15] S*,[5,6,16] and S‡,[17] has been proposed on the basis of recent experiments. Since for most of the naturally occurring carotenoids these states are expected to be located between the S_1 and S_2 states, it is likely that they may be involved in relaxation processes and even play the role of donor states in carotenoid to (bacterio)-chlorophyll energy transfer.[1,6] Moreover, the S* state has been proposed to be a precursor of ultrafast singlet−triplet homofission;[6,7,16] a similar function has been also hypothesized for the $^1B_u^-$ state.[18] Thus, the network of possible relaxation pathways in carotenoids is rather complex. In addition, to describe the relaxation processes properly, it is also necessary to include vibrational relaxation that is inevitably present.[19−22]

Besides ultrafast formation of the carotenoid triplet via homofission,[6,7,16] a subpicosecond formation of carotenoid radicals has been also demonstrated recently. In solution, a low-yield generation of the carotenoid radical from the S_2 state was observed for β-carotene[23] and lycopene[24] dissolved in chlorinated solvents. Apart from the S_2 state, the $^1B_u^-$ state was also speculated to be a potential precursor of the subpicosecond β-carotene radical formation in solution,[25] while population of a charge-transfer state has been suggested to precede carotenoid radical formation in light-harvesting complexes of purple bacteria.[9] It was also shown that on a slower, microsecond time scale carotenoid radicals can be formed from the carotenoid triplet state. This process was readily observed in both β-carotene and lycopene in chloroform sensitized by anthracene,[24,26] and explained by electron transfer from the carotenoid triplet state to chloroform.[26] However, even without anthracene

* Corresponding author. Current address: Institute of Physical Biology, University of South Bohemia, Zámek 136, CZ-337 33 Nové Hrady, Czech Republic. Telephone: +420-386-361-259. Fax: +420-386-361-219. E-mail: polivka@ufb.jcu.cz.

† Lund University.

‡ The University of Western Ontario.

10.1021/jp052227s CCC: $30.25
Published on Web 07/19/2005

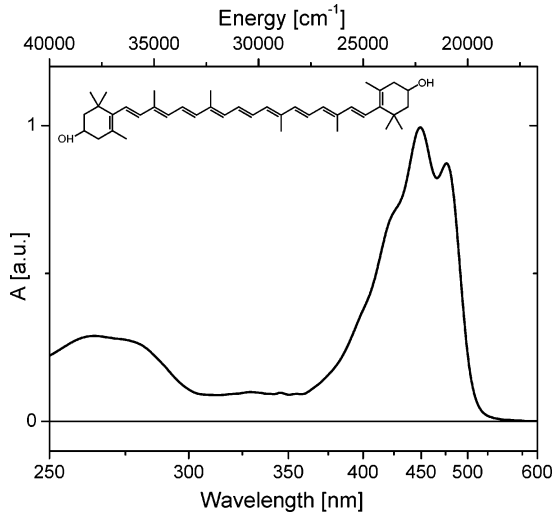

Figure 1. Absorption spectrum of zeaxanthin in methanol at room temperature. Molecular structure of zeaxanthin is shown as inset.

sensitization, excitation of the carotenoid spheroidene in methanol at 355 nm also produced the spheroidene radical on the microsecond time scale.[10]

To add to the large complexity of carotenoid relaxation pathways, it was recently shown that the relaxation pattern is excitation wavelength dependent.[17,27,28] Excitation of β-carotene to a higher vibrational state of the S_2 state even opened a new relaxation channel including the $S^{\ddagger}$ state that was not accessible by exciting the lowest vibrational levels of the S_2 state.[17] The importance of excitation wavelength in determining the relaxation pattern can be also traced from earlier studies. Despite the very low triplet yield of carotenoids, Hashimoto et al. observed a clear triplet signal after excitation of β-carotene at 355 nm,[29] while no hint of the triplet state was observed in later studies using excitation into the lowest vibrational band of the S_2 state around 480 nm.[17,20] In addition to the changes in relaxation pathways, the excess energy excitation is also expected to affect vibrational relaxation, as recently shown for β-carotene and lycopene.[28] For carotenoid radical formation, no obvious excitation wavelength dependence has been found.[25]

Thus, taking into account all the possible relaxation pathways, it is obvious that the full relaxation pattern of a carotenoid molecule is enormously complex. Aiming for better understanding of carotenoid relaxation pathways, in this study we have investigated the excitation wavelength dependence of the excited-state dynamics of the carotenoid zeaxanthin (see Figure 1 for molecular structure). This carotenoid is interesting for several reasons. First, from the spectroscopic point of view, it is in principle indistinguishable from β-carotene; thus it allows direct comparison with previous studies. On the other hand, contrary to β-carotene, the hydroxyl groups of zeaxanthin allow using polar solvent that is critical for exploring radical formation. Second, zeaxanthin is an important photoprotective molecule in various naturally occurring systems. It was recently shown that singlet excited states of zeaxanthin are likely directly involved in nonphotochemical quenching,[8,30] which is a key process in photoprotective machinery of higher plants.[3] It must be noted, however, that the precise role of the zeaxanthin excited states in this process remains unclear, as both S_1 state[30] and cation radical[8] have been proposed to be responsible for the nonphotochemical quenching. Besides, zeaxanthin is also selectively accumulated in the human retina, where, either free or protein-bound, it is also a part of the photoprotective mechanisms operating in the human eye.[31] In this study we have applied time-resolved absorption spectroscopy on a broad time scale extending from femtoseconds to microseconds. In comparison with previous studies, we have also extended the excitation wavelength dependence to electronic states lying above the S_2 state. This approach, combined with sophisticated methods of global data analysis, allowed us to extract details about the excited-state processes in the carotenoid zeaxanthin.

2. Experimental Section

Zeaxanthin (Hoffmann LaRoche) was dissolved in methanol (Merck) to achieve an optical density of ~0.25/mm (femtosecond measurements) or ~0.03/mm (nanosecond measurements) at the absorption maximum. For femtosecond transient absorption, a 2 mm quartz rotational cuvette was used to avoid degradation of the sample during measurements. For experiments in the nanosecond−microsecond time range, where quenching of the excited state by oxygen will affect the kinetics, a specially designed 1 cm quartz cuvette, which allows exchange of oxygen by argon, was used. All experiments were performed at room temperature.

Femtosecond Time-Resolved Spectroscopy. Transient absorption spectra and kinetics were obtained with a spectrometer based on an amplified Ti:sapphire laser system. Approximately 100 fs pulses were obtained from a Ti:sapphire oscillator and were amplified by a regenerative Ti:sapphire amplifier operating at a repetition rate of 1 kHz, yielding 120−160 fs pulses with an average energy of ~0.9 mJ/pulse at 800 nm. The amplified pulses were divided into two paths: one was used to pump an optical parametric amplifier for generation of excitation pulses with an energy of ~150 nJ/pulse, and the other was used to produce white light continuum probe pulses in a 0.5 mm sapphire plate. For experiments with 266 nm excitation, the part of the 800 nm beam used for pump beam was sent to a frequency tripler. The relative polarization of the pump and probe beams was set to the magic angle (54.7°). For detecting the transient absorption changes, both the probe beam and an identical reference beam were focused on the entrance slit of a spectrograph, which dispersed both beams onto a home-built dual photodiode array detection system with a spectral resolution of ~100 cm^{-1}. To be sure that there was no photochemical damage of the samples during measurement, absorption spectra were taken before and after all experiments.

Global Analysis of the Femtosecond Data. Kinetic traces collected by the diode-array detection system were fitted globally. All 512 kinetics traces recorded for each experiment have been fitted simultaneously using a multiexponential function in the form

$$S(\lambda,t) = \sum_{i=1} A_i(\lambda) \exp(-\tau_i/t) + A_\infty(\lambda) \qquad (1)$$

In this equation, i is the number of decay components, τ_i and A_i are the time constant and preexponential factor of the ith decay component, and A_∞ is a spectrum of the final, nondecaying component. The fitting also includes numerical deconvolution, the full width at half-maximum (fwhm) of the response function, and a fourth degree polynomial describing the chirp. The fitting procedure used general linear regression for the amplitudes of the exponentials and the Nelder−Mead simplex method for the rate constants, the fwhm, and the chirp polynomial. To visualize the excited-state dynamics, we assume that the excited zeaxanthin evolves according to a sequential scheme A → B, B → C, C → D. The arrows represent increasingly slower monoexponential processes, and the time constants of these processes correspond to lifetimes of the species A, B, and C. The spectral

profiles of the species are called evolution-associated difference spectra (EADS), and although they do not necessarily correspond to the pure spectra of the excited states, they provide valuable information about the time evolution of the whole system.[32]

Nanosecond Time-Resolved Spectroscopy. Transient absorption experiments were obtained with a standard nanosecond laser flash photolysis setup. The primary pump source for this system was a Nd:YAG laser, generating pulses of 8 ns duration at 1064 nm. A fourth-harmonic generator was used to produce excitation pulses at 266 nm, while a Quanta-Ray master optical parametric oscillator (MOPO) pumped by the third harmonic of the Nd:YAG laser (355 nm) was used to generate excitation pulses at 490 nm. The probe light from a xenon arc lamp (75 W) was focused to a 1 mm diameter spot overlapping the unfocused pump beam of 2.5 mm diameter. After passing through the sample, the probe light was passed through a single-grating monochromator and detected by the photomultipliers Hamamatsu R928 (detection range 300−700 nm) and R5108 (detection range 600−1200 nm). The signals were amplified and finally digitized by a transient recorder, enabling recording kinetics in time ranges varying from 20 ns to milliseconds.

3. Results

Steady-State Absorption. The absorption spectrum of zeaxanthin in methanol is shown in Figure 1. Absorption in the 380−500 nm region is due to the strongly allowed S_0-S_2 transition, which exhibits a pronounced vibrational structure with vibrational peaks located at 476 (0−0), 449 (0−1), and 424 nm (0−2). A weaker absorption band that covers the 250−290 nm spectral region is assigned to the $^2B_u^+$ state.

Femtosecond Transient Absorption. Transient absorption spectra and kinetics of zeaxanthin after excitation at 485, 400, and 266 nm were recorded in the 470−740 nm spectral window. The excitation wavelengths were selected to cover major features of the zeaxanthin absorption spectrum. At 485 nm, the lowest vibrational band of the S_2 state is selectively excited, while the 400 nm excitation is resonant with the 0−3 vibrational band of the S_2 state. Excitation at 266 nm allows direct excitation of the $^2B_u^+$ state. All 512 kinetic traces spanning the 470−740 nm region collected for each excitation wavelength were fitted globally. To visualize the evolution of the system after excitation, we present the results of the global fitting in terms of EADS (see Experimental Section). Raw data are shown in Supporting Information.

The EADS obtained after excitation of zeaxanthin into the lowest vibrational band of the S_2 state at 485 nm are shown in Figure 2. The results are essentially the same as those obtained by de Weerd et al. for β-carotene.[20] The EADS created directly after excitation exhibits a negative band at 525 nm due to S_2 stimulated emission, and ground-state bleaching below 500 nm. The increase of the signal above 700 nm is due to onset of the strong S_2-S_N signal that becomes the dominating feature of the S_2 spectrum in the near-infrared region.[33,34] The positive signal between 500 and 600 nm may be indicative of a fraction of a hot S_1 state populated within the excitation pulse, but we cannot exclude a possibility that due to limited time resolution the first EADS is slightly contaminated by a contribution from the second EADS (see below). The first EADS is within 135 fs, which thus corresponds to the S_2 lifetime, replaced by the second EADS characterized by a broad excited-state-absorption (ESA) feature. The position of this ESA band and the presence of the red tail extending up to 700 nm allow assignment of this band to the hot S_1 state.[19,20] This assignment is further evidenced

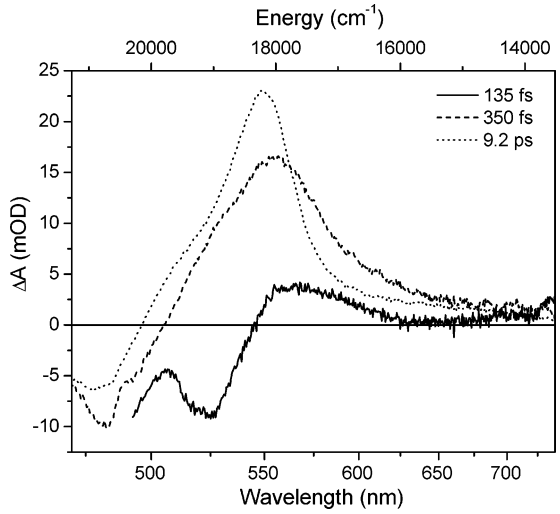

Figure 2. EADS resulting from global fitting of data obtained after excitation of zeaxanthin at 485 nm. The error margins for the time constants do not exceed ±10%, except for the fastest component for which the upper limit is ±20%.

by the change of ESA spectral profile when going from the second to the third, final EADS. This step occurs within 350 fs and is accompanied by a blue shift and narrowing of the ESA band. Both the lifetime and spectral changes are consistent with S_1 vibrational relaxation.[19,21] The final EADS has a lifetime of 9.2 ps and exhibits a typical S_1-S_N profile of zeaxanthin.[35] Therefore, it is assigned to the relaxed S_1 state that decays to the ground state with a time constant of 9.2 ps. The 510 nm shoulder clearly visible in the final EADS is due to the S* state,[6,7,16] which has in the case of zeaxanthin the same lifetime as the S_1 state.[36]

When excitation is moved to 400 nm, the EADS depicted in Figure 3 show that the decay pattern is different from that obtained after 485 nm excitation. First, the initial EADS lacks the S_2 stimulated emission band at 525 nm. Instead, stimulated emission rather occurs from higher vibrational levels, as suggested by a strong negative band around 480 nm that is due to a sum of stimulated emission and ground-state bleaching. In addition, the lifetime of the first EADS is markedly shorter, yielding 70 fs. Second, to obtain a good global fit of the data, three decay components are not sufficient: an additional decay component with a time constant of 2.8 ps is needed. Thus, contrary to the 485 nm excitation, the relaxation of the hot S_1 state (dashed line EADS in Figure 3) does not produce a fully relaxed S_1 state. Instead, the S_1-S_N ESA further narrows during the process characterized by the 2.8 ps time constant. This evolution step clearly forms the pronounced 510 nm shoulder of the S_1-S_N band whose origin has been earlier assigned to the S* state.[6,7,16] It must be noted that the 2.8 ps component is missing in the ground-state bleaching as evidenced by its zero amplitude in this spectral region (see spectral profiles of the preexponential factors in Figure 3b). Thus, although there is a slight decrease of the S_1-S_N ESA amplitude during this evolution step, it does not mean that a fraction of the molecules has 2.8 ps lifetime. Instead, this step is related solely to a relaxation process within the S_1 state and the decrease of amplitude is a consequence of fitting the data to a sequential model that cannot take into account branching relaxation schemes. The last EADS again exhibits a characteristic S_1-S_N profile and decays to zero in 9 ps.

The EADS resulting from global fitting of data obtained after excitation of zeaxanthin into the $^2B_u^+$ state at 266 nm are shown in Figure 4. Similarly to the 400 nm excitation, four components

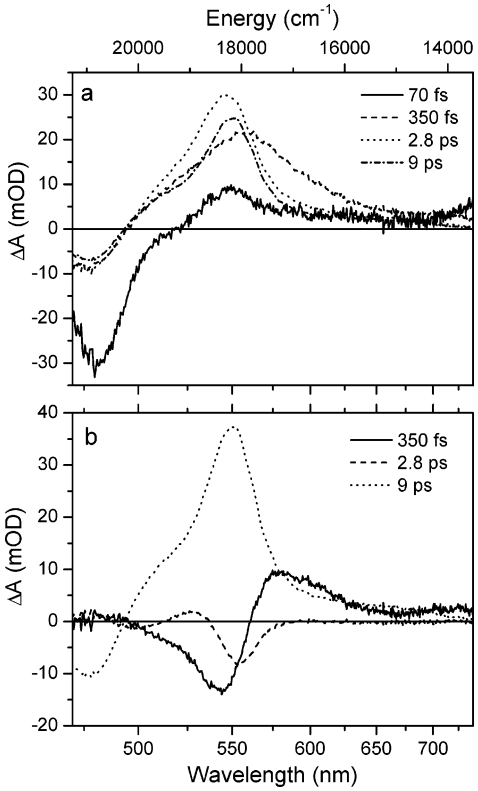

Figure 3. (a) EADS resulting from global fitting of data obtained after excitation of zeaxanthin at 400 nm. The error margins for the time constants do not exceed ±10%, except for the fastest component for which the upper limit is ±20%. (b) Corresponding spectral profiles of preexponential factors of the time components. The fastest component is omitted for clarity.

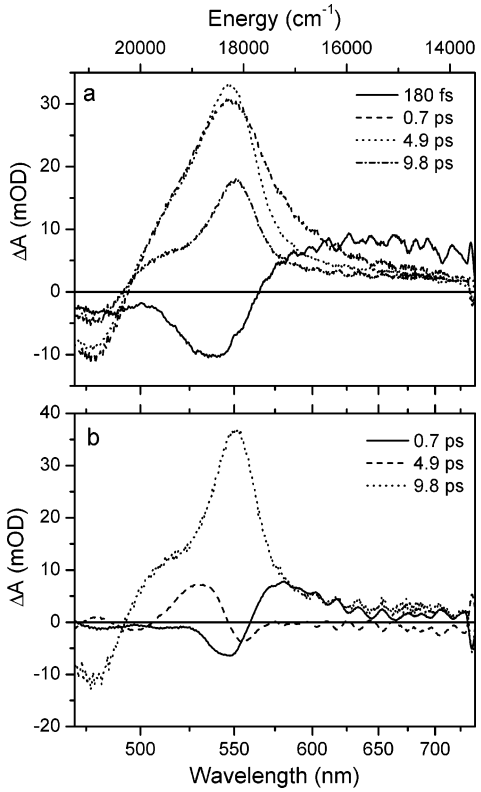

Figure 4. (a) EADS resulting from global fitting of data obtained after excitation of zeaxanthin at 266 nm. The error margins for the time constants do not exceed ±10%, except for the fastest component for which the upper limit is ±20%. (b) Corresponding spectral profiles of preexponential factors of the time components. The fastest component is omitted for clarity.

are needed to fit the data. Again, to make the assignment of the time components clearer, spectral profiles of the preexponential factors of the individual time components (see eq 1) are shown in Figure 4b. The sub-100 fs time window is obscured by a strong solvent response. The first solvent-response-free EADS (solid line in Figure 4a) resembles the EADS of the S_2 state (Figure 2). Consequently, the $^2B_u^+$ to S_2 relaxation must occur on a sub-100 fs time scale. Further evolution is similar to that observed after 400 nm excitation. The S_2 state decays in 180 fs to form a hot S_1 state (second EADS, dashed line) that further relaxes in 0.7 ps to produce the S_1-S_N band centered at 550 nm. Similar to 400 nm excitation, this S_1-S_N band further narrows on the picosecond time scale (4.9 ps) to form the final, relaxed S_1-S_N ESA consisting of the main band located at 550 nm and a blue shoulder at 510 nm. Like the picosecond component observed after 400 nm excitation (see above), the 4.9 ps process is due to an excited-state relaxation/cooling, because it has essentially zero amplitude in the ground state bleaching region (Figure 4b). The 4.9 ps component is most pronounced as a decay of the blue part of the S_1-S_N band, leading to a narrowing of the main S_1-S_N peak and formation of the 510 nm shoulder.

Nanosecond Transient Absorption. Although no long-lived products have been observed in experiments with femtosecond time resolution, earlier studies of carotenoids using picosecond−nanosecond excitation pulses found transient species with lifetimes in the microsecond time scale.[25,37] Therefore, we have measured transient absorption spectra after excitation pulses of 8 ns duration. While no long-lived transients were observed after 485 nm excitation of zeaxanthin in methanol (data not shown), a different result was obtained when zeaxanthin was excited at 266 nm. Figure 5a shows the transient absorption spectra in the 400−1000 nm region. At 2 μs after excitation, the transient spectrum has two prominent positive features at 510 and 890 nm accompanied by a ground-state bleaching at 470 nm. The 510 nm band is clearly due to the triplet−triplet (T_1-T_N) excited-state absorption, because its shape and spectral position match well those of the zeaxanthin triplet state observed earlier in toluene (524 nm)[38] and benzene (520 nm),[39−41] In the near-infrared region, the 890 nm band resembles the D_0-D_2 band of carotenoid radical cations.[9,42] The maximum at 890 nm is close to 910 nm reported for the zeaxanthin radical in benzene.[37] Thus, we assign the near-infrared band at 890 nm to the zeaxanthin radical cation. Comparing the transient spectra recorded at different delays, it is obvious that zeaxanthin triplet and radical exhibit completely different dynamics. This is depicted in Figure 5b, where kinetics taken at 440 (bleaching), 510 (triplet), and 890 nm (radical) are shown. The kinetics were fitted globally, and the results are summarized in Table 1. Most of the triplet formation is instantaneous with the used time resolution (~30 ns), but an additional 5 μs rise component constitutes ~35% of the rise. The origin of this rise component, which is also present in the 440 nm kinetics, is unknown and possible causes will be discussed in the Discussion section. Zeaxanthin triplet decays with a time constant of 25 μs, which is in the range expected for a lifetime of a carotenoid triplet state.[39] For the zeaxanthin radical, almost half of the rise is instantaneous while the rest yields a time component of 25 μs, matching the decay of the triplet state. The zeaxanthin radical decays by a second-order reaction and full decay does not occur within our time window of 1 ms; about 15% of the radical population remains at 800 μs.

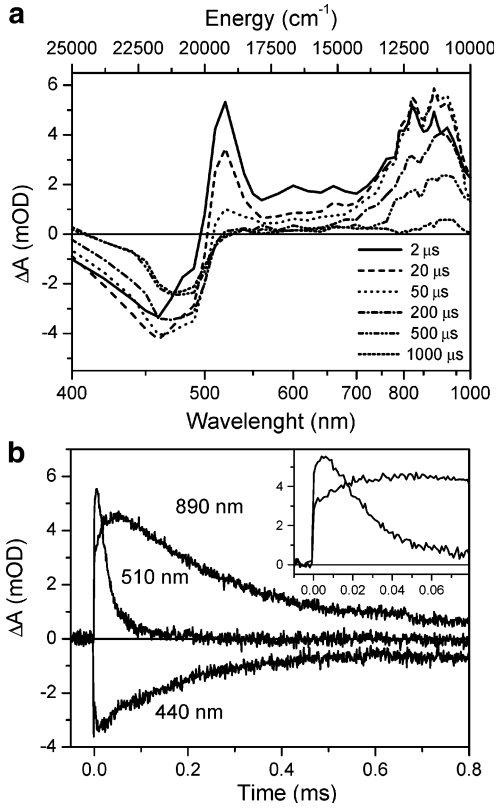

Figure 5. (a) Transient absorption spectra of zeaxanthin in the microsecond time domain produced after excitation at 266 nm by 8 ns pulses. (b) Kinetics recorded at 440 nm (ground-state bleaching), 510 nm (triplet state), and 890 nm (radical) after excitation by 8 ns pulses centered at 266 nm. Inset: decay of the triplet state and rise of the zeaxanthin radical in the first 60 μs.

TABLE 1: Global Fitting of Microsecond Kinetics of Zeaxanthin in Methanol[a]

λ_{probe} (nm)	$\tau_1 = 5\ \mu s$	$\tau_2 = 25\ \mu s$	$\tau_3 = 240\ \mu s$	$\tau_4 > 1$ ms
440	−30		84	16
510	−34	95	5	
890		−55	92	8

[a] Numbers correspond to relative amplitudes (percent) of the fitting components. Negative amplitude represents a rise; positive amplitude corresponds to decays. Excitation at 266 nm.

4. Discussion

Relaxation Dynamics After Excess Energy Excitation. The results presented here demonstrate that excitation into higher excited states of zeaxanthin adds to the complexity of the relaxation pattern. When zeaxanthin is excited into the lowest vibrational band of the S_2 state at 485 nm, the observed results match the four-state scheme ($S_2 \rightarrow$ hot $S_1 \rightarrow S_1 \rightarrow S_0$) proposed earlier.[20] The time constants of the particular relaxation processes are 135 fs (S_2 decay), 350 fs (S_1 vibrational relaxation), and 9.2 ps (S_1 decay). These values are in agreement with previous results on β-carotene or zeaxanthin employing either global[16,20] or single-wavelength analysis.[19,43] Providing excess energy by exciting the highest vibrational bands of the S_2 state generates a relaxation pattern that cannot be explained by the simple four-state scheme. First, a ~50 nm blue shift of the S_2 stimulated emission observed after 400 nm excitation as compared with 485 nm excitation (compare first EADS in Figures 2 and 3) suggests that depopulation of the S_2 state precedes the S_2 vibrational relaxation. The absence of the 525 nm stimulated emission band after 400 nm excitation implies that the relaxed S_2 state is never formed, and the hot S_1 state is populated directly by relaxation from the initially excited higher vibrational levels of the S_2 state. Thus, the hot $S_2 \rightarrow$ hot S_1 relaxation efficiently competes with the S_2 vibrational relaxation, resulting in a markedly shorter S_2 lifetime of 70 fs. Second, the subpicosecond relaxation of the hot S_1 state produced after 400 nm excitation does not produce a fully relaxed S_1 state, but an additional slower relaxation component of 2.8 ps is needed to reproduce the experimental data (Figure 3). The origin of this component cannot be assigned unequivocally on the basis of our data. It is possible that direct relaxation from the hot S_2 state excites S_1 vibrational modes that are not excited when the hot S_1 state is formed from the relaxed S_2 state. Such a situation may indeed occur as evidenced by the fact that the hot S_1 spectrum is broader after 400 nm excitation (compare second EADS in Figures 2 and 3). Then, cooling of these modes may occur on a time scale longer than that for "normal" S_1 vibrational relaxation. Another possibility is that excess excitation energy enables formation of conformers in the S_2 state. Such a mechanism has been suggested by de Weerd et al. to explain excited-state dynamics of β-carotene.[20] In such a case, a fraction of the S_2 population undergoes a conformational change. The conformational relaxation to restore the all-trans conformation occurs in the S_1 state and is characterized by the 2.8 ps time component. This explanation is consistent with the change of the shape of the S_1-S_N band during the 2.8 ps process: prior to the 2.8 ps relaxation the S_1-S_N band is rather broad and featureless, which is expected for a distribution of conformers, and the 2.8 ps process restores the relaxed shape of the S_1-S_N band.

Further changes of the relaxation pattern are observed when excitation is moved to 266 nm. The relaxation of the excited $^2B_u^+$ state occurs on the sub-100 fs time scale. Its exact time constant is not possible to determine due to interference with strong solvent signals occurring within the excitation pulse. However, a spectrum resembling the S_2 state is created within the first 100 fs (Figure 4). Contrary to the 400 nm excitation, the first EADS contains a pronounced stimulated emission band around 530 nm, suggesting that $^2B_u^+$ relaxation produces a relaxed S_2 state. Nevertheless, the stimulated emission band is markedly broader than that observed after 485 nm excitation (compare first EADS in Figures 2 and 4). This, together with a broad, featureless positive signal above 600 nm in the first EADS obtained after 266 nm excitation, again points to a possibility of formation of a distribution of conformers that is promoted by the excess energy excitation. Further relaxation is similar to that obtained after 400 nm excitation, except the time constants of the relaxation processes are longer, yielding 700 fs and 4.9 ps, respectively. The reason for this behavior has been recently suggested by Kosumi et al.,[28] who pointed out that due to the ultrafast relaxation of the higher excited states of carotenoids the excess energy excitation cannot be fully dissipated into the surroundings prior to relaxation to the S_1 state and it is rather stored in vibrational motion of the excited carotenoid molecule. Consequently, the larger excess excitation energy, the longer it takes to restore the fully relaxed S_1 state.[28]

It is worth mentioning that excited-state processes in the S_1 state occurring on the picosecond time scale have been reported earlier. A ~2 ps component was necessary to reproduce data obtained after excitation of β-carotene by 10 fs pulses.[44] Picosecond relaxation components exhibiting behavior consistent with that observed here have been also found for lycopene,[45] astaxanthin,[46] and hydroxyechinenone.[47] In the cases of astaxanthin and hydroxyechinenone, the picosecond relaxation components exhibited solvent dependence, as they were pro-

nounced only in certain solvents. The solvent dependence and the fact that these picosecond relaxation components seem to be observed solely for longer carotenoids are consistent with the hypothesis that conformation change is the primary cause of the picosecond relaxation dynamics in the S_1 state of zeaxanthin and other carotenoids.

Involvement of the "Dark" Excited States. An important question to answer is if there is a possible involvement of dark excited states, because recent studies suggested that change of excitation wavelength may open new pathways that were not accessible by excitation into the lowest vibrational band of the S_2 state.[17] The dark excited states of interest in the zeaxanthin case are the $^1B_u^-$ state that is expected to lie below the S_2 state for zeaxanthin,[18] the S* state that is visible as the 510 nm shoulder in the transient absorption spectra of zeaxanthin,[16] and finally the $S^‡$ state that has been found to be populated by excitation of the higher vibrational bands of β-carotene.[17] For the $^1B_u^-$ state, Rondonuwu et al.[18] hypothesized that the red tail of the S_1-S_N signal, readily observed on the subpicosecond time scale for most of the carotenoids studied so far (second EADS in Figures 2−4), is not due to a vibrationally hot S_1 state, but they assigned it instead to an excited-state absorption from the $^1B_u^-$ state.[18] Although such an assignment is, in principle, possible, our results do not support it. First, the changes in the spectral shape of the second EADS when going from 485 to 400 nm excitation are consistent with assignment of this band to the vibrationally hot S_1 state, because relaxation from higher vibrational levels of the S_2 state (400 nm excitation) should produce a broader hot S_1 spectrum, which is in agreement with observed experimental data (Figures 2 and 3). Second, the assignment of the second EADS peaking at ∼560 nm to the $^1B_u^-$ state causes difficulties in explaining energies of the states involved in the transition. Since the magnitude of the signal of the second EADS is comparable with that of the S_1-S_N band, the transition must be strongly allowed. Thus, if the initial state was the $^1B_u^-$ state, the final state must be of A_g^+ symmetry. The energy of the lowest state of A_g^+ symmetry is known, because it is the "cis peak" located at ∼29 000 cm^{-1} for β-carotene.[48] β-Carotene can be used for comparison, because it has the same conjugation system as zeaxanthin. Then, subtracting the energy of the observed transition (560 nm corresponds to 17 850 cm^{-1}) leads to the $^1B_u^-$ energy of 11 150 cm^{-1}, which is significantly lower than the expected $^1B_u^-$ energy of β-carotene (16 550 cm^{-1}).[14] Thus, we conclude that the second EADS corresponds to the vibrationally hot S_1 state and no spectral features attributable to the $^1B_u^-$ state are observed in our experiments.

On the other hand, the 510 nm shoulder assigned previously to the S* state is clearly visible in transient absorption spectra. The S* state cannot be distinguished from the S_1 state on the basis of lifetime, since, as shown by pump−dump−probe spectroscopy, for zeaxanthin the S* state has nearly the same lifetime as the S_1 state.[36] Interestingly, however, the intensity of the S* state shoulder varies with excitation wavelength. This is demonstrated in Figure 6, which shows normalized final EADS corresponding to the fully relaxed S_1 state. It is obvious that the S* shoulder becomes more pronounced when the excitation wavelength is moved toward higher energies. There is even a clear isosbestic point suggesting that the increase of the S* population is accompanied by a decrease of intensity of the blue part of the S_1-S_N transition. From the global analysis shown in Figures 3 and 4, it is clear that for 400 and 266 nm excitation the S* state shoulder is formed during the last relaxation step occurring on the 2.8 and 4.9 ps time scale,

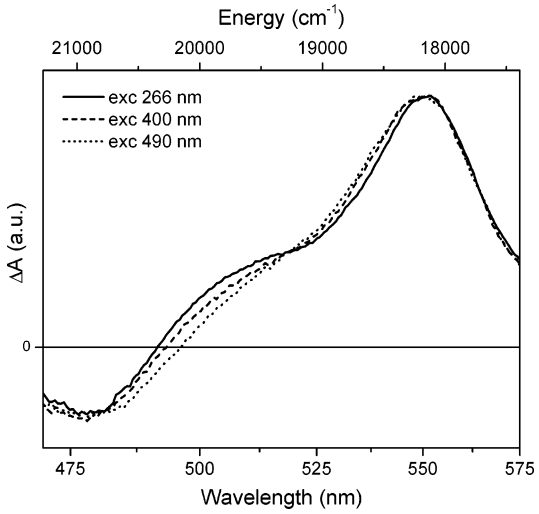

Figure 6. Final EADS corresponding to the relaxed S_1-S_N transition obtained from global fitting of the data recorded after excitation of zeaxanthin at different excitation wavelengths by pulses of ∼130 fs duration. Spectra are normalized to maximum.

respectively. Consequently, our results reveal another pathway of the S* formation that differs significantly from the sub-100 fs S_2-S^* pathway, which was the only one described so far.

The process characterized by the 2.8 and 4.9 ps components was assigned to a conformational relaxation. Since more conformers are formed with higher excitation energy (amplitude of the time component corresponding to the last relaxation step increases when going from 400 to 266 nm excitation), a feasible explanation of the observed behavior is that the conformational change of the zeaxanthin molecule is a process that promotes population of the S* state. Because these conformers end in the S* state, a corresponding decrease of the S_1-S_N excited-state absorption is observed. This scenario is consistent with the well-known fact that the S* state is more readily populated for longer carotenoids, because the longer the carotenoid is the easier the conformational change can occur. The increased population of the S* state in light-harvesting complexes of purple bacteria where the carotenoid conformation deviates from ideal all-trans configuration[49] also supports the hypothesis that conformational change of a carotenoid promotes population of the S* state. In a protein environment the S* state is a precursor of ultrafast triplet formation and the distortion of the carotenoid has been suggested to drive this process.[6,50] Our experiments suggest that conformational change is important not only for ultrafast triplet formation, but also for population of the S* state. It is worth mentioning that the suggested "conformational" mechanism of the S* state formation favors the idea of the S* state being an independent excited state rather than a vibrationally hot ground state as suggested in some studies.[36,51]

Contrary to the previous results on β-carotene in *n*-hexane,[17] we have not observed any signs of the $S^‡$ state. This state was predominantly populated after excitation into higher vibrational levels of the S_2 state and was characterized by a lifetime significantly longer than that of the S_1 state (65 ps).[17] No evidence for such a state has been found here. Global analysis of the femtosecond data did not reveal any excited-state species with lifetimes longer than 10 ps. In Figure 7 are shown kinetics recorded at a probing wavelength where the $S^‡$ signal was observed for β-carotene (510 nm). It is clear that within experimental error the kinetics are independent of excitation wavelength and, contrary to β-carotene, no long-lived species are produced after 400 nm excitation. Due to limitations caused by the available signal-to-noise ratio, we cannot rule out the

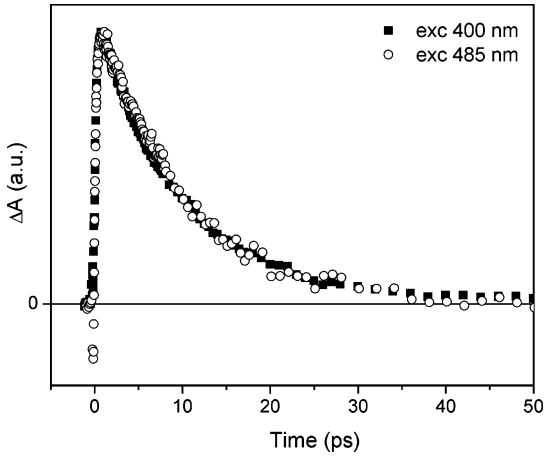

Figure 7. Kinetics recorded at 510 nm after excitation of zeaxanthin at 485 (open symbols) and 400 nm (filled symbols). Kinetics are normalized to maximum.

possibility that a long-lived component with very low amplitude (<3%) is present, but even if this were the case, the population of the $S^{\ddagger}$ state would be significantly lower than that observed for β-carotene. The origin of this discrepancy is unknown, and further studies (effects of solvent, carotenoid structure, excitation intensity, etc.) are needed to clarify the origin of the $S^{\ddagger}$ state.

Besides the increased population of the S* state at shorter excitation wavelengths discussed above, in the femtosecond−picosecond time domain we have not found any evidence for generating other species such as triplets or radicals, even after excitation into the $^2B_u^+$ state at 266 nm. All transient signals decay to zero within the first 50 ps, and although carotenoid radicals do not have a distinct signal in the 470−740 nm region used for probing, the absence of a residual bleaching signal is sufficient evidence that no long-lived products are observed. To support this conclusion further, we have measured femtosecond transient absorption kinetics at 890 nm, where the zeaxanthin radical has its peak absorption. Even with 266 nm excitation, kinetics do not possess any long-lived component attributable to zeaxanthin radical formation (data not shown). For both 485 and 266 nm excitation, the 890 nm kinetics consist of fast, ∼120 fs decay due to the S_2-S_N signal and a 9 ps component due to the high-energy tail of the S_1-S_2 excited-state absorption that extends down to 800 nm for zeaxanthin.[52] Thus, no ultrafast formation of zeaxanthin radical has been observed in methanol.

Triplet and Radical Generation by Nanosecond Excitation Pulses. The absence of long-lived signals after femtosecond excitation is in apparent contradiction to generation of the zeaxanthin radical and triplet by nanosecond pulses (Figure 5). Since we have observed the triplet and radical formation only after excitation at 266 nm, neither S_1 nor S_2 states are the precursors. Thus, the high-energy states must be involved. A possible explanation for this discrepancy is similar to that proposed by Gurzadyan et al.,[25] who observed generation of the β-carotene radical after excitation by picosecond pulses, which contradicted the absence of radicals in earlier experiments using femtosecond excitation. These authors argued that if the excitation pulse is longer than the lifetime of the excited state, the large number of photons in the excitation pulse produces a stationary population of the excited state.[25] In our experiments, when using nanosecond excitation, the number of photons per pulse is about 1 order of magnitude higher than the number of molecules in the excitation area. In such a case, it is possible that the front of the excitation pulse excites most of the molecules, creating the stationary S_1 population. Consequently, there is a nonzero probability that some of the excited molecules will interact within their S_1 lifetime with photons coming in the later parts of the excitation pulse. Using the reported zeaxanthin S_1 energy of ∼14 100 cm^{-1},[52] such a double interaction after 266 nm excitation would populate excited states lying above 50 000 cm^{-1} that may open new pathways leading to a more efficient triplet and radical formation. Although this mechanism is certainly feasible, more detailed experiments involving intensity dependence and precise measurements of the yields of the triplet and radical formation are necessary to verify this hypothesis.

Triplet and Radical Dynamics. When the zeaxanthin triplet and radical are formed, the dynamics taking place on the microsecond time scale is similar to that reported earlier for β-carotene and lycopene, whose triplet states were populated via anthracene sensitization.[24,26] The triplet state decays almost exclusively to form the zeaxanthin radical, as the triplet decay matches the radical rise and no corresponding component is observed in the ground-state recovery (see Table 1). This is the same situation as for β-carotene and lycopene,[24,26] although the time scales differ. The zeaxanthin triplet decays to form the radical with a 25 μs time constant, which is longer than the 10 [24] and 6.2 μs [26] reported for β-carotene. The discrepancy is most likely caused by slightly different experimental conditions (carotenoid concentration, different solvent), because the triplet-to-radical conversion is a bimolecular reaction involving solvent.[24,26] Therefore, we conclude that the process of triplet-to-radical conversion for zeaxanthin proceeds via the same mechanism as described in detail in previous studies of lycopene and β-carotene in chlorinated solvents.[24,26] In this work, however, we show that this process can occur even in the nonchlorinated solvent methanol and without anthracene sensitization. The triplet-to-radical conversion constitutes 55% of the total radical formation, while the rest is formed directly from the upper excited states (see above). The zeaxanthin radical decays in a bimolecular reaction to form the ground state of zeaxanthin as evidenced by the same decay component in the ground-state bleaching at 440 nm (Table 1).

The most intriguing is the 5 μs component pronounced as a rise in both triplet state and the ground-state bleaching. The rise in the bleaching region means that the component has its origin in a bimolecular reaction involving the ground-state zeaxanthin. A similar, but slower rise component in the bleaching signal was also found for β-carotene and lycopene in chloroform.[24,26] These authors attributed the component to diffusion-limited secondary reactions between chloroform radical molecules and ground-state carotenoid leading to generation of carotenoid radical. Here, however, the zeaxanthin radical cannot be involved, as the 5 μs component has no amplitude in the radical region (Table 1). Consequently, the origin of this component is interaction of some excited-state species with ground-state zeaxanthin, leading to the production of the zeaxanthin triplet. It could be speculated that singlet oxygen is involved, since the 5 μs time constant is in the range expected for singlet oxygen quenching by zeaxanthin, considering the concentration used in this study.[53] However, since we work in anaerobic conditions, singlet oxygen cannot be the source of the 5 μs triplet production. Thus, the origin of the component that accounts for about 30% of the triplet population is unclear, although excitation of solvent molecules via interaction with high-energy states of zeaxanthin populated by the double-excitation mechanism described above could be a possibility. However, this hypothesis cannot be verified on the basis of our data.

Acknowledgment. We thank Hans-Erik Åkerlund for providing us with purified zeaxanthin. The work at Lund University was supported by grants from the Swedish Research Council, the Wallenberg Foundation, and the Crafoord Foundation. T.Po. thanks the Swedish Energy Agency for financial support.

Supporting Information Available: Raw data showing transient absorption spectra at selected delay times for different excitation wavelengths. This material is available free of charge via the Internet at http://pubs.acs.org.

References and Notes

(1) Polívka, T.; Sundström, V. *Chem. Rev.* **2004**, *104*, 2021.
(2) Frank, H. A.; Cogdell, R. J. *Photochem. Photobiol.* **1996**, *63*, 257.
(3) Holt, N. E.; Fleming, G. R.; Niyogi, K. K. *Biochemistry* **2004**, *43*, 8281.
(4) Frank, H. A., Brudvig, G. W. *Biochemistry* **2004**, *43*, 8607.
(5) Hanley, J.; Deligiannakis, Y.; Pascal, A.; Faller, P.; Rutherford, A. W. *Biochemistry* **1999**, *38*, 8189.
(6) Papagiannakis, E.; Kennis, J. T.; van Stokkum, I. H. M.; Cogdell, R. J.; van Grondelle, R. *Proc. Natl. Acad. Sci. U.S.A.* **2002**, *99*, 6017.
(7) Gradinaru, C. C.; Kennis, J. T. M.; Papagiannakis, E.; van Stokkum, I. H. M.; Cogdell, R. J.; Fleming, G. R.; Niederman, R. A.; van Grondelle, R. *Proc. Natl. Acad. Sci. U.S.A.* **2001**, *98*, 2364.
(8) Holt, N. E.; Zigmantas, D.; Valkunas, L.; Li, X.-P.; Niyogi, K. K.; Fleming, G. R. *Science* **2005**, *307*, 433.
(9) Polívka, T.; Pullerits, T.; Frank, H. A.; Cogdell, R. J.; Sundström, V. *J. Phys. Chem. B* **2004**, *108*, 15398.
(10) Polívka, T.; Zigmantas, D.; Herek, J. L.; He, Z.; Pascher, T.; Pullerits, T.; Cogdell, R. J.; Frank, H. A.; Sundström, V. *J. Phys. Chem. B* **2002**, *106*, 11016.
(11) Kodis, G.; Herrero, C.; Palacios, R.; Marino-Ochoa, E.; Gould, S.; de la Garza, L.; van Grondelle, R.; Gust, D.; Moore, T. A.; Moore, A. L.; Kennis, J. T. M. *J. Phys. Chem. B* **2004**, *108*, 414.
(12) Pan, J. X.; Xu, Y. H.; Sun, L. C.; Sundström, V.; Polívka, T. *J. Am. Chem. Soc.* **2004**, *126*, 3066.
(13) Kodis, G.; Herrero, C.; Palacios, R.; Mariño-Ochoa, E.; Gould, S.; de la Garza, L.; van Grondelle, R.; Gust, D.; Moore, T. A.; Moore, A. L.; Kennis, J. T. M. *J. Phys. Chem. B* **2004**, *108*, 414.
(14) Sashima, T.; Koyama, Y.; Yamada, T.; Hashimoto, H. *J. Phys. Chem. B* **2000**, *104*, 5011.
(15) Furuichi, K.; Sashima, T.; Koyama, Y. *Chem. Phys. Lett.* **2002**, *356*, 547.
(16) Wohlleben, W.; Buckup, T.; Herek, J. L.; Cogdell, R. J.; Motzkus, M. *Biophys. J.* **2003**, *85*, 442.
(17) Larsen, D. S.; Papagiannakis, E.; van Stokkum, I. H. M.; Vengris, M.; Kennis, J. T. M.; van Grondelle, R. *Chem. Phys. Lett.* **2003**, *381*, 733.
(18) Rondonuwu, F. S.; Watanabe, Y.; Fujii, R.; Koyama, Y. *Chem. Phys. Lett.* **2003**, *376*, 292.
(19) Billsten, H. H.; Zigmantas, D.; Sundström, V.; Polívka, T. *Chem. Phys. Lett.* **2002**, *355*, 465.
(20) de Weerd, F. L.; van Stokkum, I. H. M.; van Grondelle, R. *Chem. Phys. Lett.* **2002**, *354*, 38.
(21) McCamant, D. W.; Kukura, P.; Mathies, R. A. *J. Phys. Chem. A* **2003**, *107*, 8208.
(22) Yoshizawa, M.; Aoki, H.; Hashimoto, H. *Phys. Rev. B* **2001**, *6318*, 180301.
(23) Zhang, J.-P.; Fujii, R.; Koyama, Y.; Rondonuwu, F. S.; Watanabe, Y.; Mortensen, A.; Skibsted, L. H. *Chem. Phys. Lett.* **2001**, *348*, 235.
(24) Han, R.-M.; Wu, Y.-S.; Feng, J.; Ai, X.-C.; Zhang, J.-P.; Skibsted, L. H. *Photochem. Photobiol.* **2004**, *80*, 326.
(25) Gurzadyan, G. G.; Steenken, S. *Phys. Chem. Chem. Phys.* **2002**, *4*, 2988.
(26) Fujii, R.; Koyama, Y.; Mortensen, A.; Skibsted, L. H. *Chem. Phys. Lett.* **2000**, *326*, 33.
(27) Zigmantas, D.; Hiller, R. G.; Yartsev, A.; Sundström, V.; Polívka, T. *J. Phys. Chem. B* **2003**, *107*, 5339.
(28) Kosumi, D.; Yanagi, K.; Nishio, T.; Hashimoto, H.; Yoshizawa, M. *Chem. Phys. Lett.* **2005**, *408*, 89.
(29) Hashimoto, H.; Koyama, Y.; Hirata, Y.; Mataga, N. *J. Phys. Chem.* **1991**, *95*, 3072.
(30) Ma, Y. Z.; Holt, N. E.; Li, X. P.; Niyogi, K. K.; Fleming, G. R. *Proc. Natl. Acad. Sci. U.S.A.* **2003**, *100*, 4377.
(31) Landrum, J. T.; Bone, R. A. *Arch. Biochem. Biophys.* **2001**, *385*, 28.
(32) van Stokkum, I. H. M.; Larsen, D. S.; van Grondelle, R. *Biochim. Biophys. Acta* **2004**, *1657*, 82.
(33) Zhang, J.-P.; Skibsted, L. H.; Fujii, R.; Koyama, Y. *Photochem. Photobiol.* **2001**, *73*, 219.
(34) Papagiannakis, E.; van Stokkum, I. H. M.; van Grondelle, R.; Niederman, R. A.; Zigmantas, D.; Sundström, V.; Polívka, T. *J. Phys. Chem. B* **2003**, *107*, 11216.
(35) Frank, H. A.; Cua, A.; Chynwat, V.; Young, A.; Gosztola, D.; Wasielewski, M. R. *Photosynth. Res.* **1994**, *41*, 389.
(36) Wohlleben, W.; Buckup, T.; Hashimoto, H.; Cogdell, R. J.; Herek, J. L.; Motzkus, M. *J. Phys. Chem. B* **2004**, *108*, 3320.
(37) Mortensen, A.; Skibsted, L. H. *J. Agric. Food Chem.* **1997**, *45*, 2970.
(38) Nielsen, B. R.; Jörgensen, K.; Skibsted, L. H. *J. Photochem. Photobiol., A* **1998**, *112*, 127.
(39) Burke, M.; Land, E. J.; McGarvey, D. J.; Truscott, T. G. *J. Photochem. Photobiol., B* **2000**, *59*, 132.
(40) Rodgers, M. A. J.; Bates, A. L. *J. Photochem. Photobiol.* **1980**, *31*, 533.
(41) Dallinger, R. F.; Farquharson, W. H.; Woodruff, W. H.; Rodgers, M. A. J. *J. Am. Chem. Soc.* **1981**, *103*, 7433.
(42) Jeevarajan, J. A.; Wei, C. C.; Jeevarajan, A. S.; Kispert, L. D. *J. Phys. Chem.* **1996**, *100*, 5637.
(43) Macpherson, A. N.; Gillbro, T. *J. Phys. Chem. A* **1998**, *102*, 5049.
(44) Cerullo, G.; Lanzani, G.; Zavelani-Rossi, M.; De Silvestri, S. *Phys. Rev. B* **2001**, *63*, 2411.
(45) Zhang, J. P.; Chen, C. H.; Koyama, Y.; Nagae, H. *J. Phys. Chem. B* **1998**, *102*, 1632.
(46) Ilagan, R. P.; Christensen, R. L.; Chapp, T. W.; Gibson, G. N.; Pascher, T.; Polívka, T.; Frank, H. A. *J. Phys. Chem. A* **2005**, *109*, 3120.
(47) Polívka, T.; Kerfeld, C. A.; Pascher, T.; Sundström, V. *Biochemistry* **2005**, *44*, 3994.
(48) Tsukida, K. *Methods Enzymol.* **1992**, *213*, 291.
(49) Papiz, M. Z.; Prince, S. M.; Howard, T.; Cogdell, R. J.; Isaacs, N. W. *J. Mol. Biol.* **2003**, *326*, 1523.
(50) Papagiannakis, E.; Das, S. K.; Gall, A.; van Stokkum, I. H. M.; Robert, B.; van Grondelle, R.; Frank, H. A.; Kennis, J. T. M. *J. Phys. Chem. B* **2003**, *107*, 5642.
(51) Andersson, P. O.; Gillbro, T. *J. Chem. Phys.* **1995**, *103*, 2509.
(52) Polívka, T.; Herek, J. L.; Zigmantas, D.; Åkerlund, H.-E.; Sundström, V. *Proc. Natl. Acad. Sci. U.S.A.* **1999**, *96*, 4914.
(53) Conn, P. F.; Schalch, W. Truscott, T. G. *J. Photochem, Photobiol., B* **1991**, *11*, 41.